Electronic Supplementary Information (ESI) for Journal of Materials Chemistry C
This journal is © The Royal Society of Chemistry 2018

Photophysics behind High Luminescent Two-dimensional Hybrid Perovskite $(CH_3(CH_2)_2NH_3)_2(CH_3NH_3)_2Pb_3Br_{10}$ thin films

Daniel Ramirez[a,†], José Ignacio Uribe[a,b] Luca Francaviglia[c], Pablo Romero-Gomez[c], Anna Fontcuberta i Morral[c] and Franklin Jaramillo[a,†]

[a.] *Centro de Investigación, Innovación y Desarrollo de Materiales – CIDEMAT, Facultad de Ingeniería, Universidad de Antioquia UdeA, Calle 70 No. 52-21, Medellín, Colombia.*
[b.] *Grupo de Estado Sólido, Instituto de Física, Universidad de Antioquia UdeA, Calle 70 No. 52-21, Medellín, Colombia.*
[c.] *Laboratoire des Matériaux Semiconducteurs, Institut des Matériaux, Ecole Polytechnique Fédérale de Lausanne, 1015 Lausanne, Switzerland.*
† Corresponding authors: D.R: estiben.ramirez@udea.edu.co and F.J: franklin.jaramillo@udea.edu.co

Figure S1 shows the low magnification topography and KPFM image of the 2D perovskite. The calculated work function was 5.23±0.05 eV. This result is key to designing optoelectronic devices because gives insights about band alightment conditions.

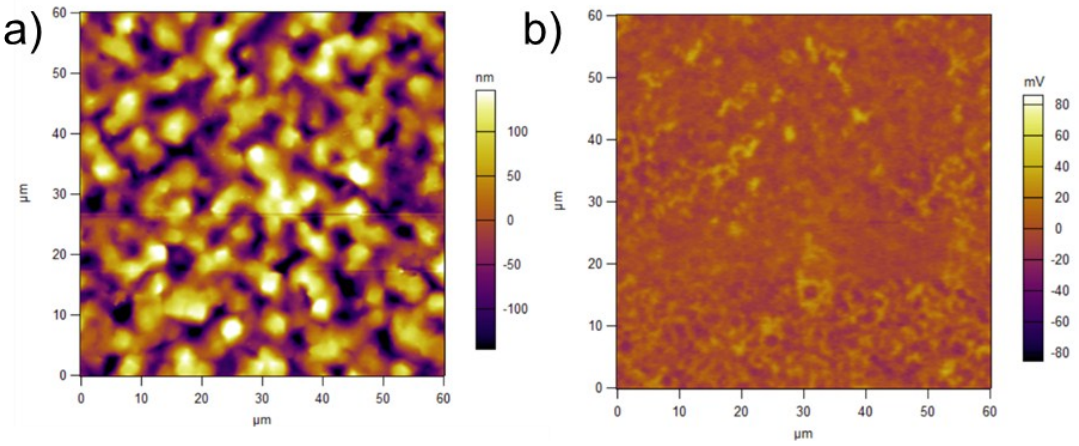

Figure S1. (a) Topography and KPFM image of the $(MA)_2(PA)_2Pb_3Br_{10}$ film.

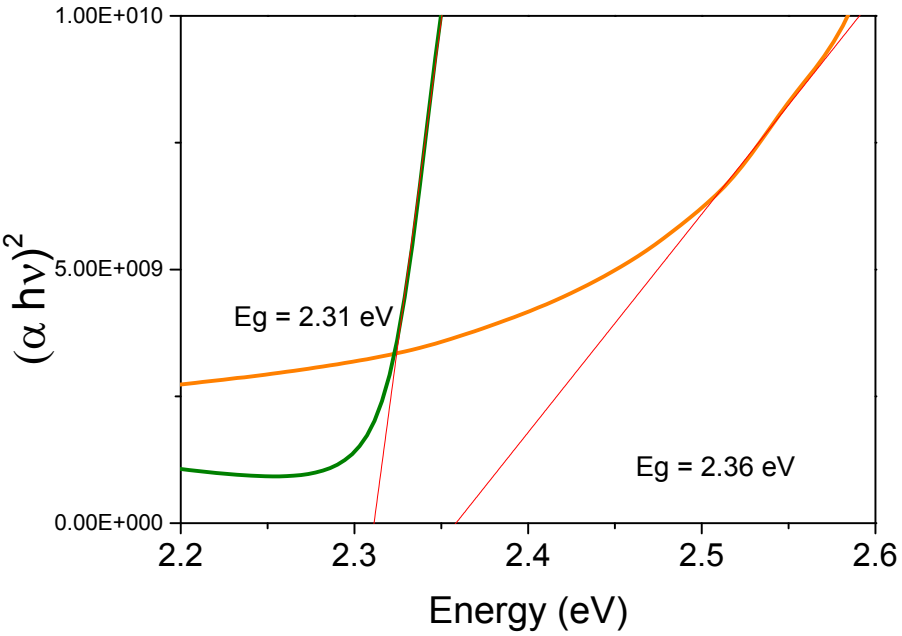

Figure S2. Tauc plots of $(PA)_2(MA)_2Pb_3Br_{10}$ (orange line) and $MAPbBr_3$ (green line) films.

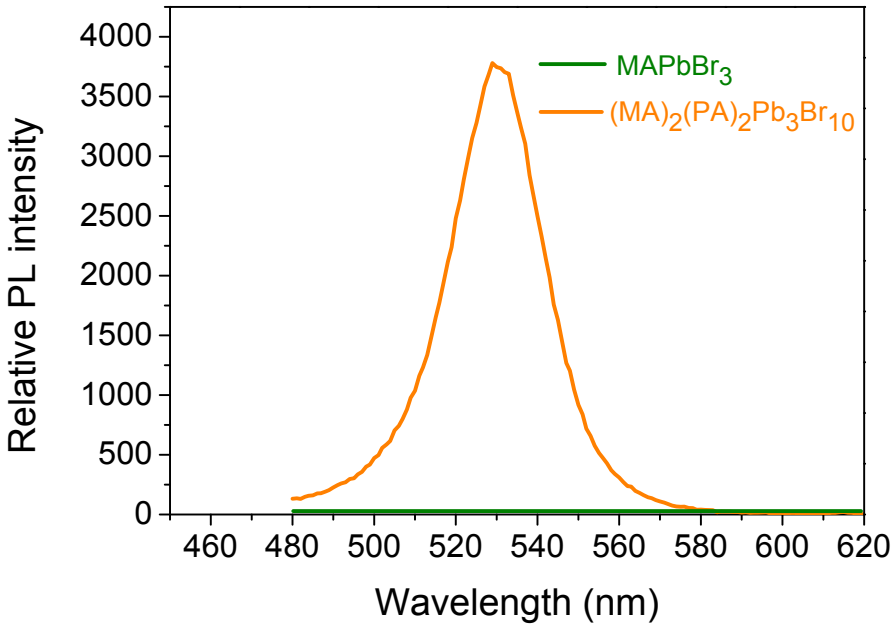

Figure S3. Room temperature PL spectrum of $(PA)_2(MA)_2Pb_3Br_{10}$ and $MAPbBr_3$ films excited at 470 nm.

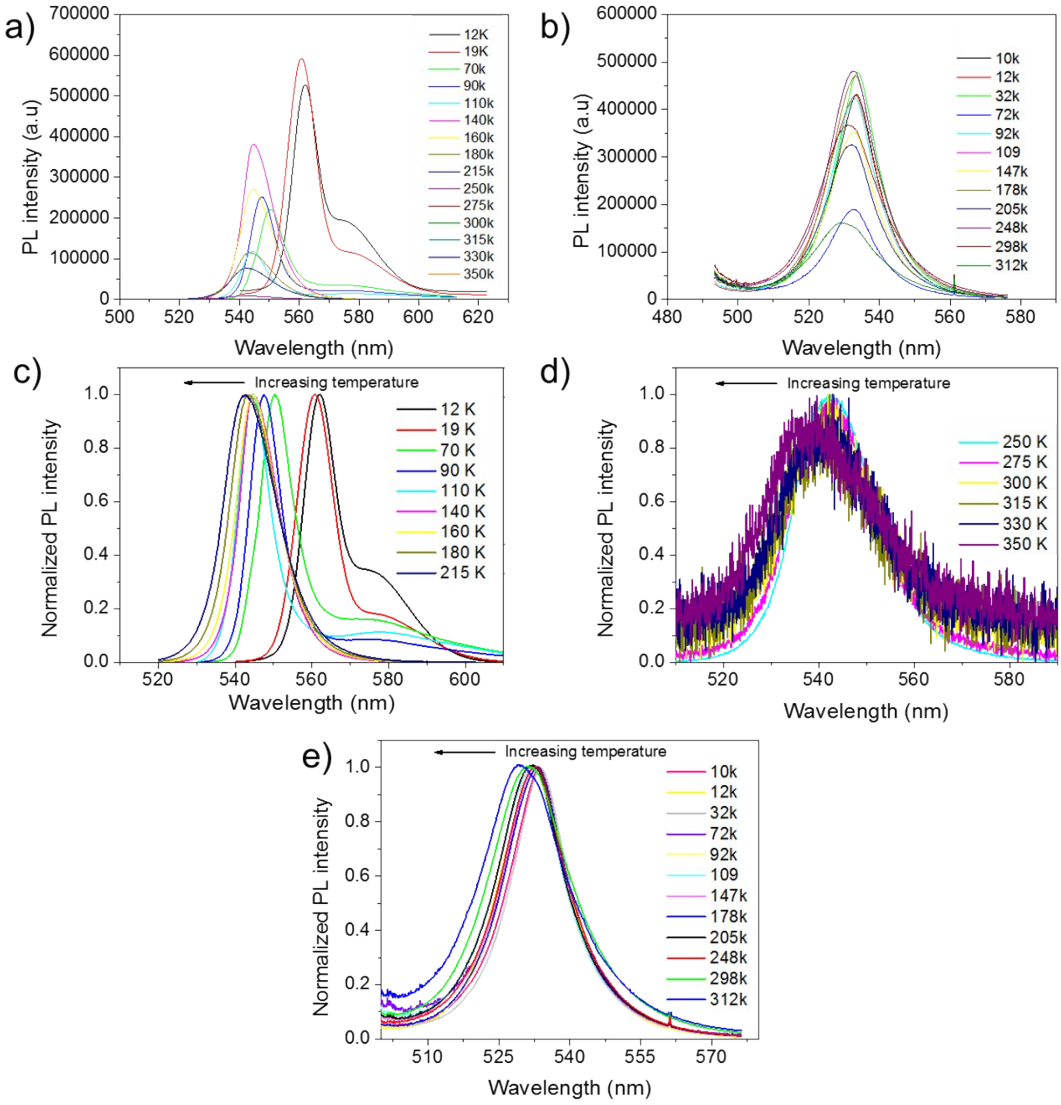

Figure S4. Temperature dependent PL spectra for (a) $MAPbBr_3$ and (b) $(MA)_2(PA)_2Pb_3Br_{10}$. Normalized PL spectra for $MAPbBr_3$ in the range of (c) 12K to 215K and (d) 250K to 350K, respectively. (e) Normalized PL spectra for $(MA)_2(PA)_2Pb_3Br_{10}$. Note that PL intensity tends to decrease as temperature increases, nevertheless, this decrease is not continuous and can be due to some untransformed room temperature perovskite phase as already previously described.[2]

Supplementary note

Different mechanisms of scattering between charge carriers and phonons or impurities are associated with different functional dependencies of the PL linewidth $\Gamma(T)$ on temperature. which can be expressed as[3]:

$$\Gamma(T) = \Gamma_0 + \Gamma_{ac} + \Gamma_{LO} + \Gamma_{imp}$$

$$\Gamma(T) = \Gamma_0 + \gamma_{ac}T + \gamma_{LO}N_{LO}(T) + \gamma_{imp}e^{\left(\frac{-E_b}{K_bT}\right)}$$

Where Γ_0 is the temperature-independent inhomogeneous broadening term, which arises from scattering due to disorder and imperfections.[4] Γ_{ac} and Γ_{LO} are homogeneous broadening terms from acoustic and LO phonon (Fröhlich) scattering, with charge-carrier-phonon coupling strengths γ_{ac} and γ_{LO}, respectively. The final term, Γ_{imp}, phenomenologically accounts for scattering from ionized impurities with an average binding energy E_b.[5] These impurities contribute γ_{imp} of inhomogeneous broadening to the width when fully ionized.[6] Electron–phonon coupling is in general proportional to the occupation numbers of the respective phonons, as given by the Bose–Einstein distribution function45,46, taken as $N_{LO} = \frac{1}{\left[e^{\frac{E_{LO}}{K_BT}} - 1\right]}$ for LO phonons, where E_{LO} is an energy representative of the frequency for the weakly dispersive LO phonon branch.[7] Most important is that is has been demonstrated, both experimental and theoretical, that the most significant contribution arises for LO phonon scattering.[3] Then we used $\Gamma(T) = \Gamma_0 + \Gamma_{LO}$ to fit our data, as shown in Figure 4b.

References

(1) de Mello, J. C.; Wittmann, H. F.; Friend, R. H. An improved experimental determination of external photoluminescence quantum efficiency. *Adv. Mater.* **1997**, *9* (3), 230–232 DOI: 10.1002/adma.19970090308.

(2) He, H.; Yu, Q.; Li, H.; Li, J.; Si, J.; Jin, Y.; Wang, N.; Wang, J.; He, J.; Wang, X.; et al. Exciton localization in solution-processed organolead trihalide perovskites. *Nat. Commun.* **2016**, *7*, 10896 DOI: 10.1038/ncomms10896.

(3) Wright, A. D.; Verdi, C.; Milot, R. L.; Eperon, G. E.; Pérez-Osorio, M. A.; Snaith, H. J.; Giustino, F.; Johnston, M. B.; Herz, L. M. Electron–phonon coupling in hybrid lead halide perovskites. *Nat. Commun.* **2016**, *7*, ncomms11755 DOI: 10.1038/ncomms11755.

(4) Rudin, S.; Reinecke, T. L.; Segall, B. Temperature-dependent exciton linewidths in semiconductors. *Phys. Rev. B* **1990**, *42* (17), 11218–11231 DOI: 10.1103/PhysRevB.42.11218.

(5) Lee, J.; Koteles, E. S.; Vassell, M. O. Luminescence linewidths of excitons in GaAs quantum wells below 150 K. *Phys. Rev. B* **1986**, *33* (8), 5512–5516 DOI: 10.1103/PhysRevB.33.5512.

(6) Absorption and photoluminescence studies of the temperature dependence of exciton life time in lattice-matched and strained quantum well systems. *Superlattices Microstruct.* **1987**, *3* (6), 657–664 DOI: 10.1016/0749-6036(87)90195-9.

(7) Evaluation of electron-phonon coupling of Al0.27Ga0.73As/GaAs quantum wells by normal incidence reflectance. *Solid State Commun.* **1991**, *79* (7), 561–565 DOI: 10.1016/0038-1098(91)90910-N.